Molecular-dynamics model for electron transfer at the electrode-electrolyte interface

J. W. Halley and Joseph Hautman

School of Physics and Astronomy, University of Minnesota, Minneapolis, Minnesota 55455

(Received 21 March 1988)

We describe a molecular-dynamics model for the calculation of the rate of electron transfer in an outer-shell electron transfer reaction at the electrode-electrolyte interface. The model consists of 216 water molecules in a box together with one iron ion that can be in either its ferrous or its ferric valence state. In previous work we have established the validity of the model for the ion in bulk aqueous solution. Here we report the algorithm for the electron transfer rate which we are using and present results using it. The results are in reasonable accord with experiment, but the calculation is not yet parameter free.

INTRODUCTION

The theory of chemical reactions at the electrode-electrolyte interface has a long history, but the main ideas used by experimental chemists arise from the theories of Marcus.[1] While these theories have been enormously influential, comparison between theory and experiment has sometimes led to marked disagreement, even in the case of relatively simple "outer sphere" electron transfer reactions.[2] While various improved theories have been suggested[3-5] concerning the possible origins of these discrepancies, it has not been possible to reach definitive conclusions.

This paper reports progress on a project to shed light on this set of questions by making a detailed calculation of the rate of a simple electron transfer reaction by computer simulation. We have chosen the ferric-ferrous electron transfer reaction at a gold electrode for study. A parallel experimental study of the temperature dependence of the reaction is being carried out[6] at Argonne National Laboratory. An advantage of choosing heterogeneous electron transfer for such a study is that the barrier height can be controlled through the potential on the electrode and thus the barrier can be lowered sufficiently so that the reaction occurs reasonably often in a molecular-dynamics simulation. The reaction was also chosen because the ion can be made aquocoordinated experimentally so that the molecular-dynamics calculation does not need to include potentials describing other ligands such as CN groups. In previous papers[7,8] we have established that our model of the ion in the bulk electrolyte gives reasonably realistic results for the coordination number of the solvation shell of both valence states of the ion and also reproduces whatever information is available about the vibrational spectrum of the solvation shell of the ions quite well. The model for water is the Toukan-Rahman molecular-dynamics model[9] that contains a full description of the internal modes of the water molecules (treated classically). In the calculations reported here and in Refs. 7 and 8 we had 216 water molecules and one ion in the molecular-dynamics sample. The potentials between the ion and the water used in the work reported here were the potentials called "empirical" in Ref. 7.

In this paper we report our first results on the electron transfer rate itself using the molecular-dynamics model developed in the work described in Refs. 7 and 8. To produce these results required a model for the electrode surface and a quantum-mechanical model for the electron transfer process itself. In the work reported here we are using a relatively crude model for the surface and focus our attention on the second aspect: the algorithm for describing the electron transfer process. A more refined model of the electrode will be reported elsewhere.

Our algorithm of the electron transfer rate is entirely in the spirit of existing theories of electron transfer by Marcus[1] and others.[10-15] We are particularly indebted to the work of Warshel,[16,17] who has used a similar approach.

In the next section we describe our algorithm and the third section gives results. The last section contains discussion.

DESCRIPTION OF THE ALGORITHM

We assume that the electron transfer process is rapid compared to any motion of the reactant (here the iron ion) and that the motion of the ionic nuclei is purely classical. The wave functions describing the electrons of the system when the ion is in state 1 (2) are denoted $\Psi_{1(2)}$, respectively. (This is sometimes called the "tight-binding" formulation of the electron transfer problem.) These wave functions depend parametrically on the positions $\{\mathbf{R}_i(t)\}$ of the atoms in the electrolyte. The wave function $\Psi(t)$ of the system is written in the form

$$\Psi(t) = c_1(t)\Psi_1 + c_2(t)\Psi_2 . \tag{1}$$

The time-dependent Schrödinger equation is written

$$i\hbar\frac{\partial\Psi}{\partial t} = H\Psi , \tag{2}$$

where H is the electronic part of the Hamiltonian in the Born-Oppenheimer approximation and also depends on $\{\mathbf{R}_i\}$. We multiply this equation by $\Psi_{1(2)}^*$ and integrate on the electonic coordinates. Neglecting $\int\Psi_1^*\Psi_2$ and the time dependence of the $\Psi_{1,2}$ arising from the $\mathbf{R}_i$ when

taking the time derivative one finds

$$i\hbar \begin{bmatrix} \dot{c}_1 \\ \dot{c}_2 \end{bmatrix} = \begin{bmatrix} E_1(t) & \Lambda_{12}(t) \\ \Lambda_{12}(t) & E_2(t) \end{bmatrix} \begin{bmatrix} c_1 \\ c_2 \end{bmatrix} \tag{3}$$

in which $E_{1(2)}(t) = \int \Psi_{1(2)}^* H \Psi_{1(2)}$ and $\Lambda_{12}(t) = \int \Psi_1^* H \Psi_2$ and the integrals are over electronic coordinates. The

time dependence of the $E_{1,2}$ comes from the dependence of the electronic energies on the atomic positions. We suppose that at time $t = 0$, $c_1(t=0) = 1$, $c_2(t=0) = 0$ and work to lowest order in Λ_{12}. Then by changing to an appropriately defined "interaction representation" (see Appendix A) we find that the probability $|c_{1\to2}(t)|^2$ that the ion has changed from state 1 to state 2 if it started in state 1 at time t_0 is given by the following expression:

$$|c_{1\to2}(t)|^2 = \left| \int_{t_0}^{t+t_0} \frac{-i\Lambda_{12}}{\hbar} \left[\exp\frac{i}{\hbar} \int_{t_0}^{t_0+t'} [E_1(t'') - E_2(t'')]dt'' \right] dt' \right|^2 . \tag{4}$$

In this expression we estimate the energies E_1 and E_2 as the potential energies of the ion if it is in state 1 and if it is in state 2 in the same atomic positions. Thus in estimating $E_{1,2}$ we make use of the fact that the potentials used in the molecular-dynamics simulation to obtain the forces on the atoms and ions arise from the electronic state of the system in the Born-Oppenheimer sense. Λ_{12} may be regarded as the electron transfer matrix element. In our preliminary calculations we took Λ_{12} to be constant but we also report results for a position-dependent function Λ_{12} below. In Appendix B we show that this expression gives the Landau-Zener expression for the probability in the case that the energy difference $E_1 - E_2$ increases linearly with the time. Appendix B also describes some other special cases of Eq. (4) and its physical meaning in more detail.

We start the classical simulation with the ion in one of its charge states, say Fe^{2+}. At each step in the classical simulation of the trajectories we determine whether the energy difference $E_1 - E_2$ is in a "mixing region"[12] defined by the inequality $|E_1 - E_2| < E_c$ where E_c is the reciprocal of a dephasing time after which the quantum-mechanical phase coherence described by Eq. (4) is lost.[18] This time must be longer than the time for a sound wave to propagate across the molecular-dynamics sample. For a given overpotential we use the last requirement to determine E_c: Specifically, we set a time τ_c and then set E_c so that τ_c is the average time during which $|E_1 - E_2| \le E_c$ at that overpotential. We find that the reaction rates calculated as described below are essentially independent of the value of τ_c for large enough τ_c in this definition of the mixing region. As the ion enters the mixing region defined in this way, we begin calculation of the quantity $|c_{1\to2}|^2$ as given by Eq. (4). The calculation of $|c_{1\to2}|^2$ continues for succeeding time steps until the system moves out of the "mixing region" in the sense that $|E_1 - E_2|$ becomes larger than E_c. Call the value of $|c_{1\to2}|^2$ after the crossing P_1. Start calculating $c_{1\to2}$ again when the system passes back into the mixing region and continue until the next crossing out of the mixing region. When the crossing occurs calculate P_2 and so forth for N_t trials. Then the rate constant is $k_{1\to2} = (1/T)\sum_{i=1}^{N_t} P_i$. T is the total run time. One can see that this procedure should give the rate constant by noting that, from the usual formulation[19,20] [see, for example, Eq. (2.4) of Ref. 19], the rate constant is $k_{1\to2} = -dN_1/dt |_{t=0}$ where N_1 is the (nonequilibrium) value of the occupation number for state 1 of the ion and where we assume, as in our simulations, $N_1(t=0) = 1$ and $N_2(t=0) = 0$.

RESULTS

Here we report results using a code which implements this algorithm for 216 water molecules and an iron ion in an unrepeated box surrounded by soft walls. The potentials describing the interaction of the wall with the water are as follows:

$$V_{O\text{-wall}}(x) = \frac{0.265}{|x - x_0|^9} - \frac{0.028}{|x - x_0|^3} ,$$

$$V_{H\text{-wall}}(x) = \frac{0.265}{|x - x_0|^9} .$$

The units of energy are $e^2/\text{Å}$. x_0 is the position of the "wall." The interactions between the oxygen and hydrogen components of the water molecules are described in Ref. 9. The interaction between the iron ion and the water is described in Refs. 7 and 8. The ion was fixed at 8 Å from the wall in the simulations reported here. This distance corresponds to fixing the coordination shell of the ion so that it just touches the first monolayer of water at the surface. A full calculation of the rate requires that the ion be placed at a variety of starting positions and allowed to move. These features will be added to the calculation later as described in the discussion of the last section. They are not required for the tests of the basic features of the algorithm which are reported here.

Characteristic results for δE as a function of simulation time are shown in Fig. 1 (top, dark curve). These calculations were done for 9000 steps with 4.0×10^{16} sec./step. The calculated reaction rates are reproducible in successive runs. The probability $|c_{1\to2}|^2 = P$ is shown as the lower, dashed curve for two values of E_c. The electrostatic effects of charging the walls are not yet realistic so we have simulated the effect of the electrode potential by adding a constant ΔE_0 to $E_1 - E_2$. (We can estimate the average values of E_1 and E_2 from long runs when the ion is in each of the two valence states.) In Fig. 2 we show results for the "potential," that is ΔE_0 depen-
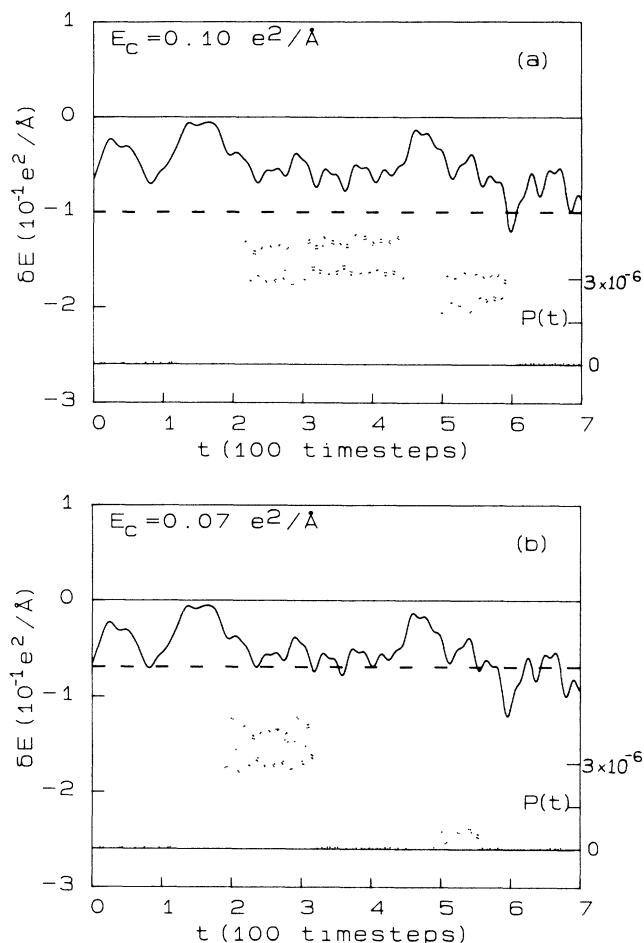
FIG. 1. Calculations of the energy difference $\delta E = E_1 - E_2$ as a function of time (top, dark curves) and of the probability P of transition to state 2 according to Eq. (4) (lower, dotted curves). δE is the same in (a) and (b). The value of E_c used to calculate P according to the algorithm discussed in the text is different (dashed line). In Figs. 1–3 we have taken $\Lambda_{12} = 10^{-5} e^2/\text{Å}$.
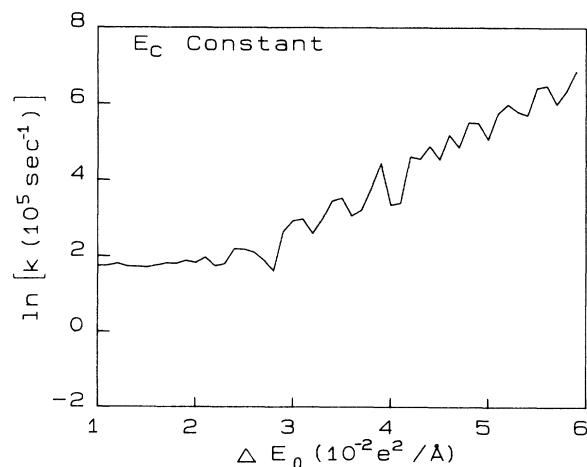
dence of the rate as calculated with constant Λ_{12} and E_c fixed for all potentials at the value 0.1 $e^2/\text{Å}$ (rather than by fixing τ_c as described above). With this procedure, the rate is not really exponential in the potential as expected and observed experimentally. On the other hand, in Fig. 3 we show the result of fixing τ_c instead of E_c so that we are using the algorithm described in the previous section. Now the potential dependence of the rate has the expected exponential form, and we can calculate a value of the parameter α which characterizes the slope as $\alpha/k_B T$. With Λ_{12} constant as in the calculations which resulted in Fig. 3, the result is $\alpha \approx 0.3$. The value is somewhat smaller than the one reported experimentally.[21] While the experimental results are based on analysis of a pulsed experiment which may require further refinement, it is interesting to explore the effects of lifting the assumption that Λ_{12} is constant in our model. In Fig. 4 we show the result of repeating the calculation of the rate with the assumption that $\Lambda_{12} = \Lambda_0 \exp(-|\delta E|/\eta)$ where, in the results shown, $\eta = 0.02$ $e^2/\text{Å}$. With this choice, the calculated rate gives a value of α which is quite consistent with $\frac{1}{2}$.

Finally we have made a preliminary exploration of whether the "crossings" at which $\delta E = 0$ in this model correspond to excursions of the A_{1g} coordinate associated with the breathing mode of the octahedron of water surrounding the ion toward the value which it takes when $\delta E = 0$ and no other displacements of the octahedron have occurred. This is the behavior expected if the A_{1g} coordinate is the "reaction coordinate" associated with the reaction, as is often supposed in applications of Marcus theory.[2] In Fig. 5 we show a graph of δE versus the A_{1g} coordinate $R_{A_{1g}}$ for one of the calculations from which the data of Figs. 2–4 were collected. If the A_{1g} coordinate is the reaction coordinate then one expects that, as $\delta E \rightarrow 0$ then the trajectory of the system in this plane should follow the dark line in Fig. 5. One sees that, though this sometimes occurs, it does not always do so.

FIG. 2. Reaction rate as a function of "overpotential" ΔE_0 calculated using an algorithm in which E_c is fixed independent of ΔE_0. The resulting rate is not exponential in ΔE_0.
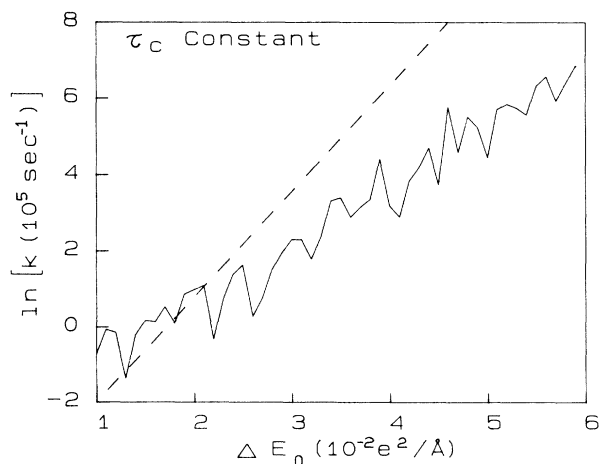

FIG. 3. Same as Fig. 2 except that the value of E_c changes with ΔE_0 in order to keep the time τ_c during which $|\delta E| \leq E_c$ fixed as discussed in the text. The calculated rate is now exponential in ΔE_0. Here τ_c is 0.7 ps. A line with slope $\alpha/k_B T = 1/2 k_B T$ is shown for reference.
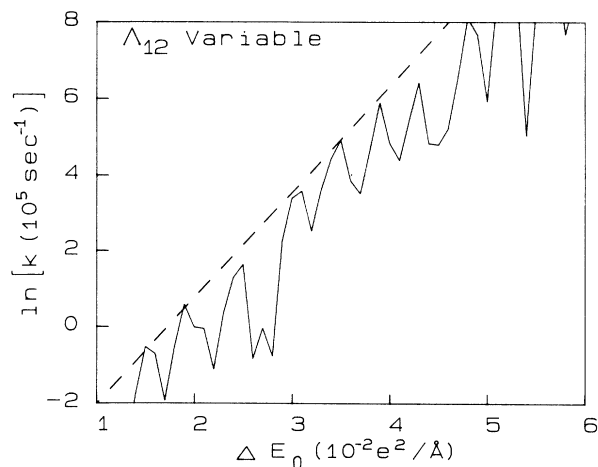
FIG. 4. Same as Fig. 3 except that the matrix element Λ_{12} is now made dependent on δE as discussed in the text (with $\Lambda_0 = 10^{-5}$ $e^2/\text{Å}$) instead of being constant as in Figs. 2 and 3. The transfer coefficient associated with the slope of $\ln k$ vs ΔE_0 is now near one-half (dashed line).

FIG. 6. Fourier-transform squared of the energy difference $\delta E(t)$ showing regions of metal oxygen (MO) stretch, water libration, water scissors modes (HOH) and OH stretch (OH) frequencies.

Some zero crossings seem to be associated with configurations which are not simply related to the A_{1g} breathing mode. What configurations these are and how important they are is still under study.

Another interesting feature of our results is that the high-frequency dynamics of the water molecules in the solvation shell, including the OH stretching modes and the HOH scissors and libration modes, may be playing a role in the dynamics of the electron transfer process. This is suggested by the high-frequency oscillations of the probability P which are evident in Fig. 1. The shortest period of these high-frequency oscillations is the period of the OH stretch frequency of the water molecule. Unfortunately, quantum-mechanical effects are significant in these high-frequency modes, so that the present classical calculation cannot describe these effects accurately. The librational and scissors motions of the water are also

present in the temporal variation of $\delta E(t)$ as can be seen from the Fourier transform of $\delta E(t)$ which is shown in Fig. 6. The lower-frequency librational and scissors modes are treated somewhat better by our classical model, though quantum-mechanical effects are probably still playing some role. We have the preliminary impression that the low-frequency part of the spectrum in Fig. 6 is not determining the calculated reaction rate, as suggested by some models of homogeneous electron transfer reactions. This question, however, requires further study.

DISCUSSION AND CONCLUSIONS

We have shown that the application of the proposed tight-binding algorithm for calculation of electron transfer reaction rates can reproduce basic qualitative features of the ferrous-ferric heterogeneous electron transfer rate such as exponential dependence on the overpotential with a transfer coefficient close to one-half when it is applied to a (rather oversimplified) molecular-dynamics model of the metal-electrolyte interface. This resolves some basic issues concerning the relation of the calculation to the observed rates, by showing, for example, that the sampling time τ_c must be held fixed as the overpotential is varied in order to obtain reasonable results. On the other hand, we found that the potential dependence of the rates was very sensitive to the form chosen for the dependence of the matrix element Λ_{12} on the atomic coordinates.

In future work, we will extend the "box" model considered here by reproducing the cell an infinite number of times in the two directions parallel to the metal surface by Ewald techniques. This will permit a more electrostatically realistic simulation. Second, we plan to allow the ion to diffuse away from the surface, in order to take the effects of ion motion and the distribution of ion-electrode distances at which electron transfer takes place into account. Third, we have begun in collaboration with
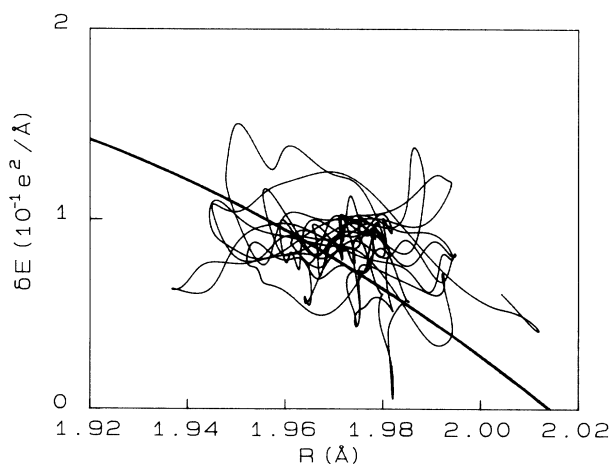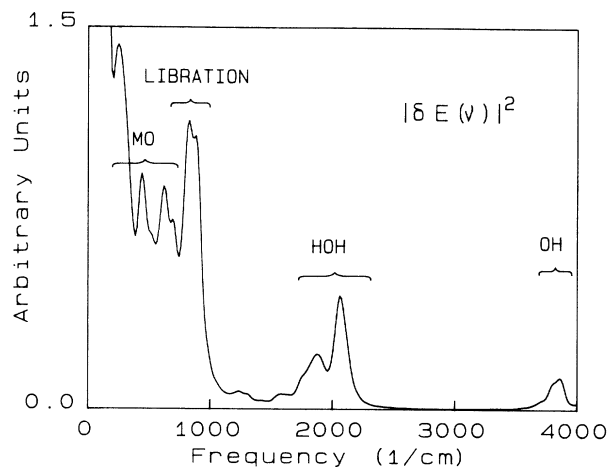

FIG. 5. δE vs the traditional reaction coordinate $R_{A_{1g}}$ for a molecular-dynamics run. The dark line shows the expected trajectory near $\delta E = 0$ in the traditional theory.

L. Curtiss to obtain more realistic forms for the dependence of Λ_{12} on atomic coordinates and will employ them in these simulations. Finally, we are interested in exploring the effects of the high-frequency modes of the water by including quantum effects on atomic motion in the simulation.[22-23]

APPENDIX A: DERIVATION OF EQ. (4)

Equation (3) is solved by introducing the coefficients $b_{1,2}$ of an interaction representation by the equation

$$c_{1,2} = b_{1,2} \exp\frac{-i}{\hbar} \int_0^t dt' E_{1,2}(t') \ . \tag{A1}$$

Inserting this into Eq. (3) gives

$$i\hbar \dot{b}_2 = \Lambda_{12} b_1(t) \exp\frac{-i}{\hbar} \int_0^t dt' [E_2(t') - E_1(t')] \ .$$

This can be integrated from $t = 0$ to time t. Assuming that $b_2 = 0$ at time 0 and using the fact that to lowest order in Λ_{12}, b_1 can be set equal to its initial value of 1 on the right-hand side of the last equation one finds that to lowest order in Λ_{12}

$$|c_2|^2 = |b_2|^2 = \left| \frac{-i\Lambda_{12}}{\hbar} \int_{t_0}^{t+t_0} \exp\left[\frac{i}{\hbar} \int_{t_0}^{t_0+t'} [E_1(t'') - E_2(t'')]dt'' \right] dt' \right|^2 \ ,$$

which is Eq. (4).

APPENDIX B: SOME LIMITING CASES OF EQ. (4)

First consider the case $E_1 - E_2 = \overline{\delta E}$, a constant. Then the integrals are easily done and one finds

$$|c_2|^2 = \frac{4\Lambda_{12}^2}{\overline{\delta E}^2} \sin^2\left[\frac{\overline{\delta E}t}{2\hbar} \right] \ .$$

Averaging over a period of the oscillating term one obtains

$$P_1 = |\bar{c}_2|^2 = \frac{2\Lambda_{12}^2}{\overline{\delta E}^2} \ ,$$

which is just the result expected from stationary perturbation theory.

Secondly, consider the case in which $\delta E(t) = \dot{\delta E}t$ so that δE is increasing linearly in time. Then inserting this into Eq. (4) gives

$$P_2 = |c_2|^2 = \frac{2\pi\Lambda_{12}^2}{\hbar \dot{\delta E}} \ ,$$

which is the Landau-Zener result[24,25] in the nonadiabatic limit.

We can qualitatively understand some features of our numerical results in terms of a sum of contributions from these two limits. Because δE has a finite average in time, we can consider that there is a contribution of the type P_1 so that, by use of our algorithm there will be a contribution of the rate of approximately

$$k_{\text{back}} = N_c P_1 / T \ , \tag{B1}$$

where N_c is the number of times δE passes within E_c of 0. This contribution arises from the mixing of the two states over long times when their energy is very different and is irrelevant to the real reaction rate. It depends on the

damping time τ_c. The nonexponential character of the results in Fig. 2 can be qualitatively understood as arising from a large contribution from this term that arises at large overpotentials at fixed E_c. When τ_c is fixed at a large value, then the contribution of this term does not increase strongly with overpotential and the spurious effects of the term are not seen in the results (as in Fig. 3).

By study of the Landau-Zener limit we can understand the relation of our results to the theories of Marcus and others in more detail. If we write the contribution to the reaction rate from each time δE passes through zero in terms of P_2 we obtain a contribution to the reaction rate from these processes of approximately

$$k_{\text{act}} = N_x P_2 / T \tag{B2}$$

in which N_x is the number of times that δE passes through zero during the run. In the theories of Marcus[26]
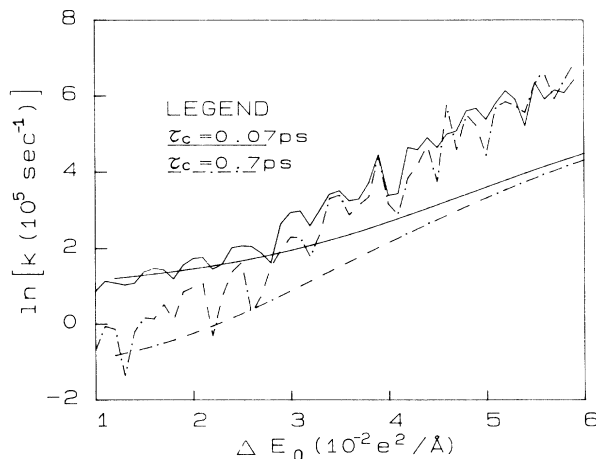

FIG. 7. Comparison of the rate calculated by the molecular-dynamics algorithm with rate obtained by summing Eqs. (B1) and (B2) of Appendix B.
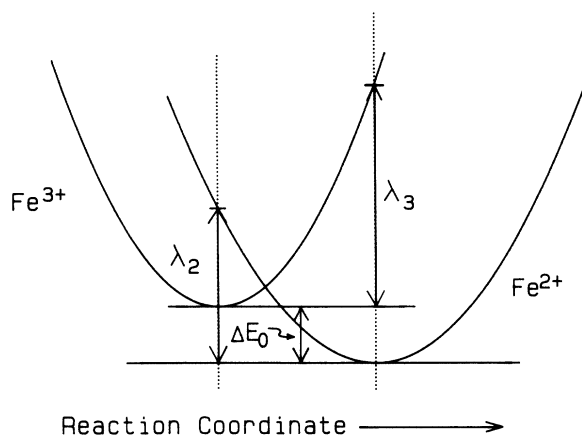
FIG. 8. Sketch of parabolic levels in the traditional model for definition of terms.
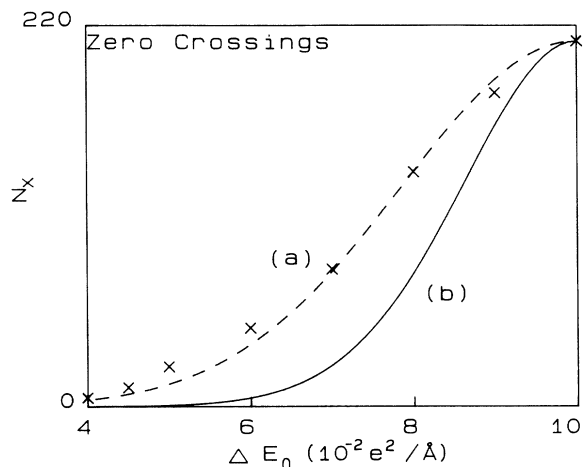

FIG. 9. Comparison of the actual number of zero crossings observed in the molecular-dynamics simulation (crosses) with the number of zero crossings as estimated from the traditional theory for the parameters of this model [curve (b)]. Curve (a) is a fit of the molecular-dynamics results to the form $\exp[-\gamma(\Delta E_0 - \lambda_2)^2]$.

and Levich and Dogonadze[27] this is precisely the approach used. It amounts to assuming there is no quantum coherence between zero crossings as well as that the only contribution to the rate is from the region near the crossing where the energy difference δE is linear in the time. In Fig. 7 we compare the result of summing the approximate expressions (B1) and (B2) with the calculation from Eq. (4) of the rate. Here we used a fit to the number N_x of zero crossings taken from the molecular-dynamics simulation itself in Eq. (B2) (see Fig. 9). One sees that the approximations seriously underestimate the rate at large overpotentials. While we do not have a complete analysis of the reason for this, it appears to arise because the effects of quantum interference between zero crossings or near zero crossings can be correlated.

Finally we can compare the number of zero crossings N_x as calculated from the molecular-dynamics simulation with the result of the traditional theories of Refs. 26 and 27. In those theories one assumes that the energy surfaces are parabolic in the reaction coordinate r as sketched in Fig. 8. The number of zero crossings N_x is supposed to be exponential in the barrier height E_b which is given in terms of the rearrangement energies λ_2 and λ_3 defined in the figure as

$$E_b = \frac{\lambda_2^2 \lambda_3}{(\lambda_3 - \lambda_2)^2}\left\{1 - \left[1 - \left[\frac{\lambda_3}{\lambda_2} - 1\right]\left[\frac{\Delta E_0}{\lambda_2} - 1\right]\right]^{1/2}\right\}^2$$

so that

$$N_x = N_0 e^{-E_b/k_B T} .$$

Here N_0 is the number of times δE would pass through zero if the barrier height were zero, or as one sees from the preceding equation within the traditional model, the

number of times that δE passes through zero if ΔE_0 were equal to λ_2. We can use these expressions to calculate the value of N_x predicted in our model by the traditional theories by. estimating the energies λ_2 and λ_3 from the molecular-dynamics runs. When the forces are calculated using the potentials appropriate to the Fe^{3+} ion, we obtain $\lambda_2 = \Delta E_0 - \overline{\delta E}$ where the bar indicates the time average over the run. Similarly when the forces are calculated from the Fe^{2+} potentials we get $\lambda_3 = \overline{\delta E} - \Delta E_0$. In our simulations we find $\lambda_2 = 0.1$ $e^2/\text{Å}$ and $\lambda_3 = 0.2$ $e^2/\text{Å}$. The values of N_x calculated from the traditional theory and from the molecular-dynamics run are compared in Fig. 9. One sees that the values of N_x predicted by the traditional model are too low. The values of the rate predicted by the traditional theory at comparable overpotentials (Fig. 7) are also too low. Thus there are two sources of discrepancy between the traditional theory and our simulation. On one hand, the effects of phase coherence enhance the effective probability of reaction at a crossing in the simulation. On the other hand, the effective number of crossings is higher in the simulation, possibly because some events are occurring in which δE is near zero even though the state is of higher energy than the one associated with the lowest saddle point on a path through the phase space which carries one from one energy minimum to the other. We are exploring this possibility further in our current work.

[1]R. A. Marcus, J. Chem. Phys. **43**, 679 (1965).
[2]J. T. Hupp and M. J. Weaver, J. Phys. Chem. **89**, 2795 (1985).
[3]W. Nadler and R. A. Marcus, J. Chem. Phys. **86**, 3906 (1987).
[4]M. D. Newton and N. Sutin, Annu. Rev. Phys. Chem. **35**, 437 (1984).
[5]J. N. Onuchic, J. Chem. Phys. **86**, 3925 (1987).
[6]N. C. Hung and Z. Nagy, J. Electrochem. Soc. **134**, 2215 (1987).

[7]L. A. Curtiss, J. W. Halley, J. Hautman, and A. Rahman, J. Chem. Phys. **86**, 2319 (1987).

[8]J. W. Halley and J. Hautman, Ber. Bunsenges. Phys. Chem. **91**, 491 (1987).

[9]K. Toukan and A. Rahman, Phys. Rev. B **31**, 2643 (1985).

[10]N. S. Hush, J. Chem. Phys. **28**, 962 (1958).

[11]B. E. Conway, J. Electroanal. Chem. **128**, 81 (1981).

[12]H. Frauenfelder and P. G. Wolynes, Science **229**, 337 (1985), and references therein.

[13]J. C. Tully and R. K. Preston, J. Chem. Phys. **55**, 562 (1971).

[14]D. P. Ali and W. H. Miller, J. Chem. Phys. **78**, 6640 (1983).

[15]R. E. Cline and P. G. Wolynes, J. Chem. Phys. **86**, 3836 (1987).

[16]A. Warshel, J. Phys. Chem. **86**, 2218 (1982).

[17]A. Warshel and J.-K. Huang, J. Chem. Phys. **84**, 4938 (1987).

[18]A detailed discussion of some subtle issues here is in A. J. Leggett *et al.*, Rev. Mod. Phys. **59**, 1 (1987).

[19]D. Chandler, J. Chem. Phys. **68**, 2959 (1978).

[20]D. Chandler, J. Stat. Phys. **42**, 49 (1986).

[21]Z. Nagy (private communication).

[22]H. L. Friedman and M. D. Newton, J. Electroanal. Chem. **204**, 21 (1986).

[23]E. Buhks, M. Bixon, J. Jortner, and G. Navon, J. Phys. Chem. **85**, 3759 (1981).

[24]L. Landau, Phys. Z. Sowjetunion **2**, 46 (1932).

[25]C. Zener, Proc. R. Soc. London, Ser. A **137**, 696 (1932).

[26]R. Marcus, J. Chem. Phys. **56**, 863 (1956).

[27]V. G. Levich and R. R. Dogonadze, Collect. Czech. Chem. Commun. **26**, 293 (1961).